NASA TN D-1681

TECHNICAL NOTE

D-1681

MECHANICAL IMPEDANCE STUDY OF THE X-259 ROCKET MOTOR

Raymond G. Hartenstein and
William G. Elsen

Goddard Space Flight Center
Greenbelt, Maryland

NATIONAL AERONAUTICS AND SPACE ADMINISTRATION
WASHINGTON June 1963

MECHANICAL IMPEDANCE STUDY OF THE X-259 ROCKET MOTOR

by
Raymond G. Hartenstein and
William G. Elsen
Goddard Space Flight Center

SUMMARY

The impedance analysis of the X-259 rocket motor and roll-rig firing assembly presented in this report indicates that the roll rig gives a soft spring effect to the rocket motor which, if unaccounted for, could lead to the misinterpretation of vibration levels especially in the higher frequency range. The mechanical impedance concept has proved to be a straightforward and plausible method of analyzing this phenomenon and, at the same time, increases the general usefulness of static firing data.

To define the static firing arrangement completely, a study of the thrust cell mounted against the firing bay wall was also made. This study revealed the dynamic character of the thrust cell and provided excellent correlation with the design parameters of the device.

CONTENTS

MECHANICAL IMPEDANCE STUDY OF THE X-259 ROCKET MOTOR

by
Raymond G. Hartenstein and
William G. Elsen
Goddard Space Flight Center

INTRODUCTION

To achieve a realistic laboratory simulation of in-flight vibration levels, an exact knowledge of the dynamic behavior of both rocket and payload is needed. The mechanical impedance concept offers this knowledge in a very useful form. Another dimension, force, is added to the dynamic picture by this concept, which allows a kinetic investigation that is more thorough than the limited kinematic approach used in the past. Mechanical impedance is a measure of the mechanical system's response (motion) to an applied excitation (force). It is in fact exactly equal to the ratio of the applied force to the resulting velocity at a point (or what may be assumed to be a point) in a structure. Instrumentation systems have been developed sufficiently so that impedance data are now being gathered on the upper-stage solid rocket motors—namely, the X-259 and X-248 manufactured by Allegany Ballistics Laboratory, Cumberland, Maryland, used as third and fourth stages of NASA Scout Vehicles. These data, in conjunction with subsequent payload impedance data measured in the laboratory, will permit the determination of more accurate environmental test levels.

This report sets forth the data and findings of an initial study, conducted January 20, 1962, of the X-259 rocket motor (Serial No. HPC-7) mounted in a special static firing fixture called a "roll rig," the purpose of which is to allow the measurement of motor roll torques during firing.

THRUST CELL – FIRING BAY WALL COMBINATION

The thrust cell, essentially a very stiff spring placed between the nose of the rocket bottle and the bay wall (test bay no. 2 at ABL), is designed to measure the thrust of the rocket motor during burning. (The thrust cell used was a 20,000-pound Baldwin L-H cell SR-4, Type TXX, Serial No. Z1009.) This cell is of considerable interest, since the impedance it presents to the rocket bottle affects to a large extent the dynamic motion, and hence acceleration, of the rocket bottle during burning. (Refer to Appendix A.)

The impedance tests on the thrust cell were expected not only to provide information on the spring constant of the thrust cell but also to give a picture of any idiosyncrasies present over the frequency range of interest.

The curve given in Figure 1 for impedance versus frequency of the thrust cell shows clearly its springlike characteristic, which holds well until 2 kc. Above 2 kc the device approaches its major resonance, which is clearly established at 3 kc. Beyond 3 kc for a small region the curve tends to approach the mass line represented by the armature (see Figure 3).

The very minor dip in the impedance curve at 1500 cps is of little significance not only because it represents a small magnitude variation but, more importantly, because it is not accompanied by any great phase change, as may be seen in the Figure 2 curve of the impedance phase angle versus frequency. Inasmuch as this dip is at half the frequency of the major resonance, it probably is a subharmonic.

The major resonance at 3.0 kc checks well with a theoretical value of 3.1 kc if the cell consists basically of the arrangement shown in Figure 3.

A thorough study of the thrust cell data revealed that it functions very nearly as expected. The equivalent circuit shown in Figure 3, with mass and spring constant values as indicated, will accurately simulate the thrust cell response up to 3 kc. The region above 3 kc is, presently at least, of little interest; this is fortunate, since both the magnitude and angle of impedance begin to perform in an extremely irrational manner above 3 kc. Some of the variation above 3 kc may, of course, be due to high frequency nonuniformities of the instrumentation system itself.

Thus we can write the thrust cell impedance for the region below 3 kc as

$$Z = \frac{k}{j\omega}\left[1 - \left(\frac{\omega}{\omega_n}\right)^2\right] ,$$

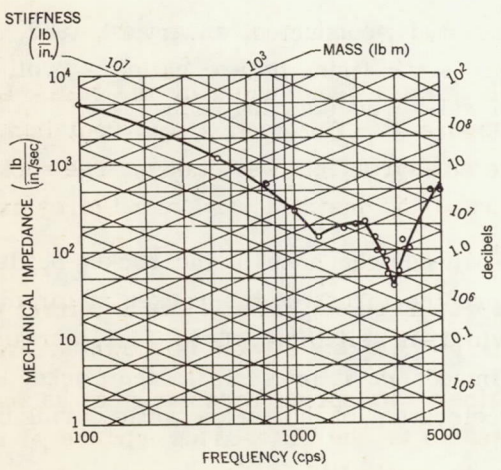

Figure 1—Impedance vs. frequency for the Baldwin L-H thrust cell.

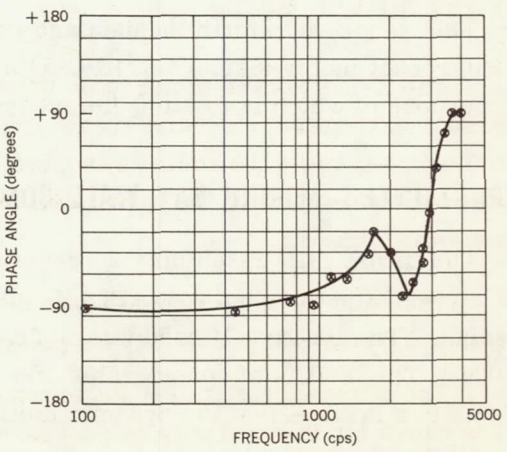

Figure 2—Phase angle vs. frequency for the Baldwin L-H thrust cell.

where k = the spring constant in lb/in. and, for a 20,000 lb thrust cell, $\omega_n = 2\pi \times 3\text{kc} = 19 \times 10^3$ rad/sec.

The damping of this system may be read directly from the impedance curve. The damping, probably due to friction, is of some significance, being equal to 40 lb/in./sec, and is read from the impedance curve in Figure 1 as the magnitude of impedance at resonance (3 kc). It can, however, be neglected for most engineering calculations (certainly below 1 kc).

The damping is included for correctness of the present analysis, and the impedance function takes the form

$$Z = D - \frac{jk}{\omega}\left[1 - \left(\frac{\omega}{\omega_n}\right)^2\right] .$$

The above equation then is an adequate representation of the thrust cell impedance between 0 and 3 kc, and will be used in general to simulate dynamically the static firing restraint system.

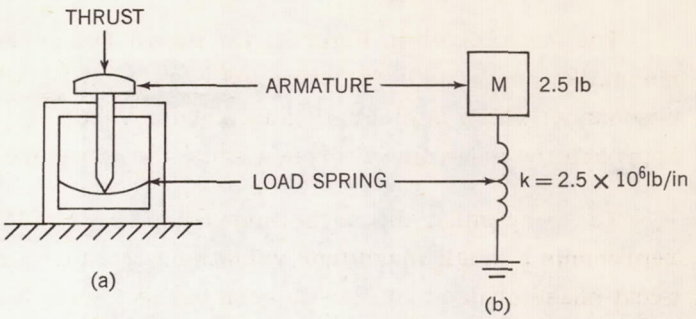

Figure 3—Thrust cell (a) Functional schematic (b) Mechanical equivalent circuit.

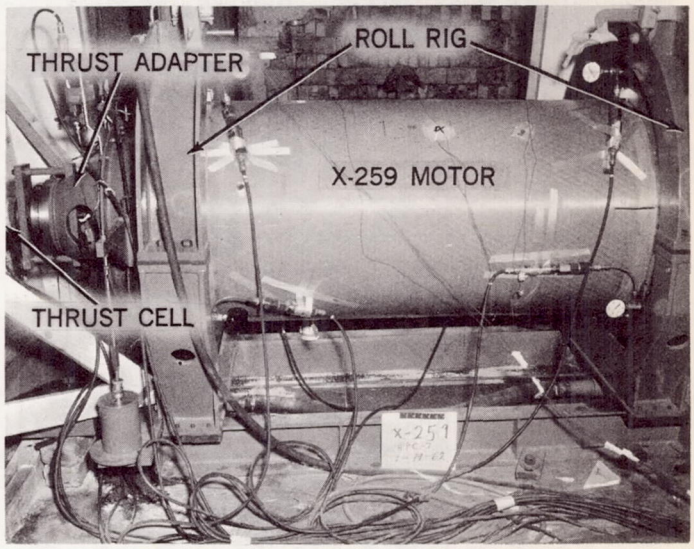

Figure 4—X-259 motor and roll-rig assembly.

X-259 ROCKET MOTOR

The X-259 rocket motor was mounted in a roll-rig fixture constructed by the NASA Langley Research Center for special rocket firing studies (see Figure 4). The system was kept intact; and, immediately after the rocket was fired, these impedance measurements were taken. The rocket motor was backed away from the thrust cell to allow installation of the instrumentation and force exciter as shown in Figure 5.

The point of contact chosen was the bearing surface which, during firing, was in direct contact with the thrust cell previously discussed. The impedance plot for this system is shown in Figure 6.

The impedance plot as a whole tends to follow a rather soft spring constant line, as indicated. The cause for this can only be postulated but is suspected to be the oil bearing surface of the roll rig. This tendency is unfortunate in a sense, since the soft spring likeness "swamps out" to a large degree modes and resonances of the bottle that are also of interest. However, the primary purpose of this test was to define the impedance characteristics of the entire system as presented to the force generated in the rocket.

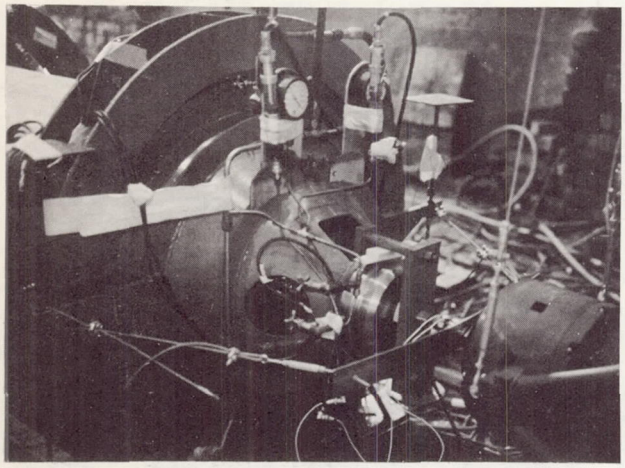

Figure 5—Impedance test arrangement.

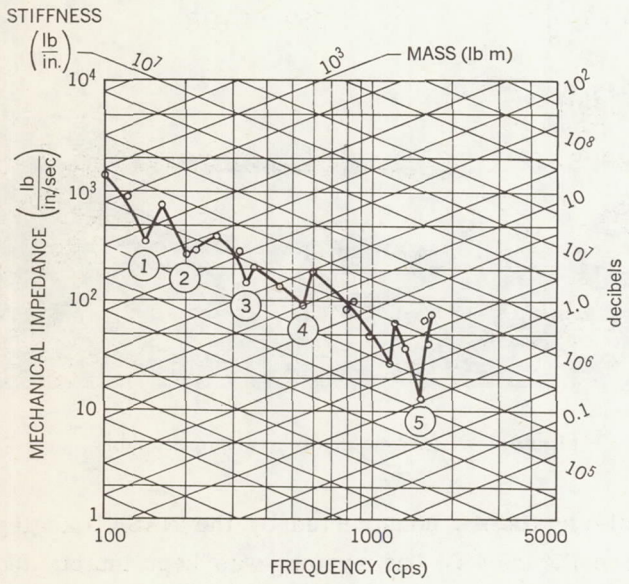

Figure 6—Impedance vs. frequency for the X-259 mounted in roll rig.

A study of the impedance plot of Figure 6 indicates five departures from the springlike characteristic. Of these, only three are significant: numbers 2, 4, and 5. The notches at 150 cps and 350 cps represent either minor structural resonances or, possibly, weak acoustical modes in the motor cavity; neither is accompanied by an appreciable phase shift, as seen in Figure 7.

Regions 2, 3, 4, and 5 of Figure 6 all represent previously identified* resonant burning modes of the X-254 motor.† Regions 2, 4, and 5 are accompanied by large phase shifts about zero degrees.

The notches (resonances) that always precede the peaks (antiresonances) are in each case preceded by a phase shift through zero degrees with a positive slope. Likewise, the peaks, or antiresonances, are always accompanied by the negative-going angle through zero degrees, which substantiates theory very well. The phase angle remains, as would be expected, at very nearly −90 degrees all other times and thus verifies the overall soft spring characteristic of the impedance plot in Figure 6.

In order to present an impedance equivalent for this system, the importance of the three departures from the springlike characteristic must be considered. Certainly, for random vibration levels, these three regions are sufficiently narrow to be given little attention. However, for considering sinusoidal levels, there may be sufficient reason for their inclusion, particularly when resonant burning conditions are to be simulated.

If we choose to neglect all but the dominant feature of these data, the impedance of

*"Information and Preliminary Data on the Scout ST-2 Launching, Sections A&H," NASA Langley Research Center letter to Chance Vought, June 26, 1961.

"Preliminary Flight Test Results of Scout ST-4," NASA Langley Research Center, March 8, 1961.

†The X-254 motor is identical to the X-259 mechanically with the exception of fuel type and configuration. Since we are considering an empty bottle, they are equivalent.

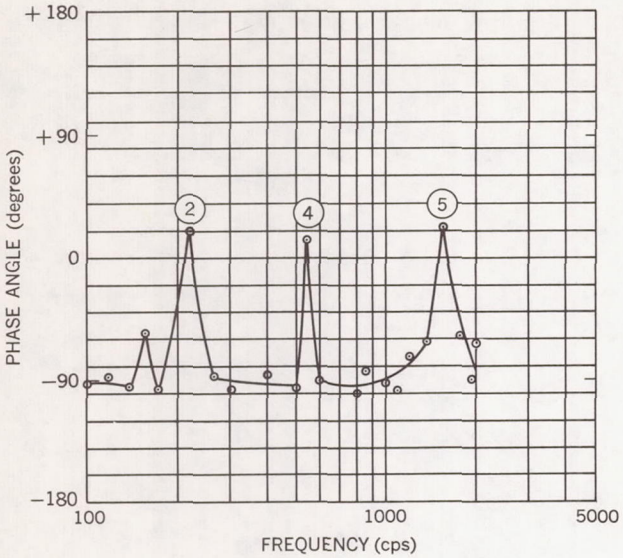

Figure 7—Phase angle vs. frequency for the X-259 and roll rig.

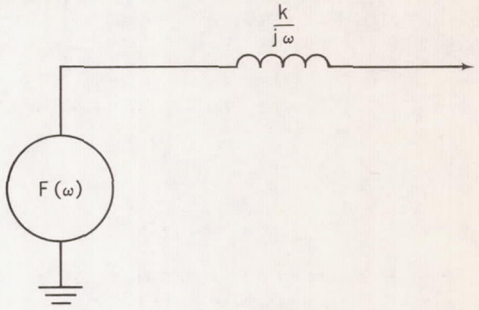

Figure 8—Impedance equivalent of the X-259 and roll rig.

the X-259 rocket motor and roll-rig combination may be established as that of a spring, or

$$Z = \frac{k}{j\omega};$$

and the equivalent impedance circuit for the entire device is as shown in Figure 8.

STATIC FIRING EQUIVALENT IMPEDANCE

To establish completely the dynamic relation between rocket motor, roll rig, and thrust cell, it is necessary simply to combine the previously found equivalent impedance for these systems. Connecting these impedance circuits of Figures 3 and 8 gives the Figure 9 circuit.

The terminating or load impedance (labeled point 1 in Figure 9) as seen by the forward collar of the rocket has a great effect on the motion at this point. This effect is directly proportional to frequency because of the springlike character of the X-259 roll-rig assembly. It must be noted that the high frequency limit placed on this circuit is 1500 cps because of the radical departure beyond this point of the impedance of the roll-rig assembly. Further studies must be made before a clear definition of the region above 1500 cps can be established.

Solving for the impedance at point 1 of Figure 9 gives

$$Z_\sigma = \frac{k_1}{j\omega}\left(\frac{k_2 - \omega^2 M}{k_1 + k_2 - \omega^2 M}\right),$$

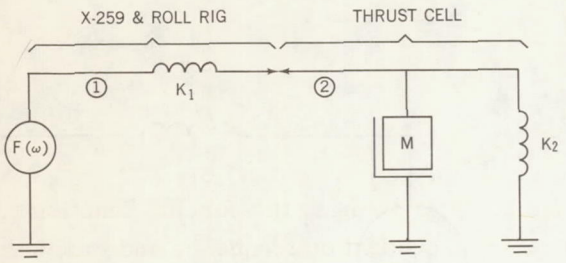

Figure 9—Impedance equivalent of the X-259 static firing assembly.

which below 2 kc may be closely approximated as

$$Z_\sigma = \frac{1}{j\omega}\left(\frac{k_1 k_2}{k_1 + k_2}\right); \qquad (1)$$

or the net effect of the entire system at point 1 is that of a spring of stiffness

$$K_{eff} = \frac{k_1 k_2}{k_1 + k_2} .$$

Equation 1 may then be written

$$Z_\sigma = \frac{K_{eff}}{j\omega} . \qquad (1a)$$

The impedance Z_σ is that presented to the force generator shown in Figure 9. The point of connection between the force generator and Z_σ (point 1) can be assumed to exist physically at the forward collar of the X-259 motor, according to our previous approximations.

It would be extremely desirable to know the function $F(\omega)$ because it represents a property that, together with the motor impedance, describes wholly the dynamic behavior of the X-259 rocket motor. This function may be found analytically as follows:

By definition,

$$F(\omega) = V(\omega) \times Z_\sigma(\omega) ;$$

and also, in order to use acceleration data, since

$$V(\omega) = \frac{A(\omega)}{j\omega} ,$$

$F(\omega)$ may be written as

$$F(\omega) = \frac{A(\omega)}{j\omega} \times Z_\sigma(\omega)$$

Assuming the frequency dependence is obvious,

$$F = \frac{AZ_\sigma}{j\omega} , \qquad (2)$$

and substituting Equation 1a into 2 gives

$$F = \frac{AK_{eff}}{-\omega^2} \cdot \tag{3}$$

With the aid of Equation 3 and acceleration data from static firings, the forcing function F, or $F(\omega)$, may be established. The function $F(\omega)$ is, as indicated, dependent on frequency and to some degree will be time-dependent as well. The time dependency results from the steady decrease of fuel mass during burning, along with a corresponding increase in chamber dimensions. This function can be measured and accounted for quite readily.

After the forcing function $F(\omega)$ and the static firing arrangement impedances have been established, the acceleration levels for other terminating impedances may be determined by analyzing the circuit of Figure 10.

It is assumed here that the payload - rocket motor configurations do not appreciably affect the forcing function $F(\omega)$ as previously found by Equation 3. The impedance of the rocket motor Z_B and the impedance of the payload Z_P will need to be firmly established. The X-259 and X-248 rocket motors are presently being studied by NASA and others.*

Since the payload configurations vary considerably, the impedance Z_P in each instance must be determined. The summation of the complex impedances $Z_B + Z_P$ can be accomplished efficiently on an analog computer with curve-following plotters.

The predicted flight level accelerations could then be established, since

$$A = j\omega \frac{F}{Z_{eq}} , \tag{4}$$

where

$$Z_{eq} = Z_B + Z_P .$$

Flight levels can then be compared with those derived from Equation 4, and regions of error can be established to increase the accuracy of subsequent predictions.

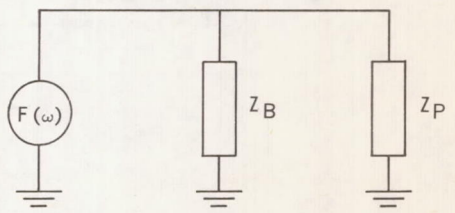

Figure 10—Equivalent impedance circuit for the rocket and payload combination.

INSTRUMENTATION AND ANALYSIS

The impedance tests all were run at Allegany Ballistics Laboratory, Ridgely, West Virginia, on January 20, 1962.

*Belsheim, R. O., and Harris, J. J., "Apparent-Weight Measurements of Rocket Payload and Test Structures," Naval Research Laboratory Memorandum Report 1099, Dec. 1960.

The equipment needed for these tests was mounted in a mobile trailer that also provided a work area. The data recording schematic is shown in Figure 11. The tape recorder provided permanent records that were returned to Goddard Space Flight Center for thorough analysis. In order to make a preliminary analysis, an oscillograph recording of a slow sine sweep was made; and from this the areas of interest (peaks and valleys) could be quickly verified. Many points were taken in these areas during the discrete frequency tests to define fully each peak or valley. The force and acceleration signals from the impedance head were carried through 100 feet of driven shield triax cable into the instrumentation van, where they were amplified, monitored, and recorded. After amplification these signals were returned to the test bay so that the control console operator also could monitor them conveniently.

The structures were excited through the impedance head by means of an electrodynamic shaker system suspended from an overhead crane, as shown in Figure 12.

This shaker system is capable of approximately 150 pounds force but was operated at a force level of 20 pounds for the thrust cell study and 70 pounds for the motor tests. The lower force level for the thrust cell tests was necessary to avoid extreme acceleration levels at resonance and yet provide a constant force level that would simplify analysis procedures.

Minor noise and pickup problems that existed in the instrumentation system were traced to faulty input connectors on the high input impedance signal conditioners used. This, however, presented only slight analysis difficulties because the signals had to be filtered in any case, to eliminate extraneous structural noises.

The impedance data analysis consisted of playing back the tape recordings through the instrumentation shown in Figure 13.

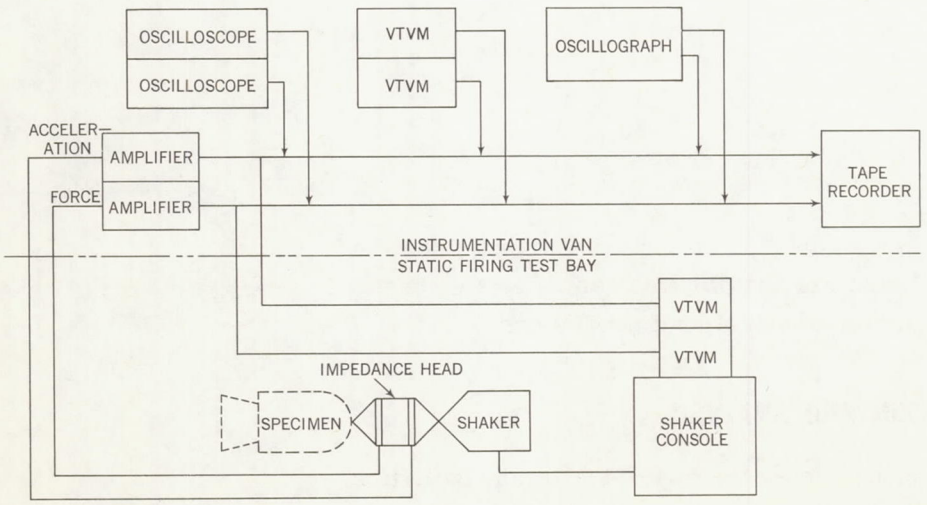

Figure 11—Instrumentation diagram for impedance measurements.

The rms voltmeter readings of the filtered force and acceleration signals were recorded, and quotients were taken to provide magnitude values of the apparent weight function as discussed in Appendix A. The phase angle values necessary to describe fully the apparent weight vector were found from the phase meter reading of the filtered signals. (These filters were compared with each other for filter-induced phase shift, and no difference was found between them.) The apparent weight data could then be plotted on the special impedance graph paper from which either impedance or apparent weight could be read. To plot the impedance phase angle, it was necessary simply to add 90 degrees to the apparent weight values, since impedance is a function of velocity rather than acceleration (discussed in Appendix A).

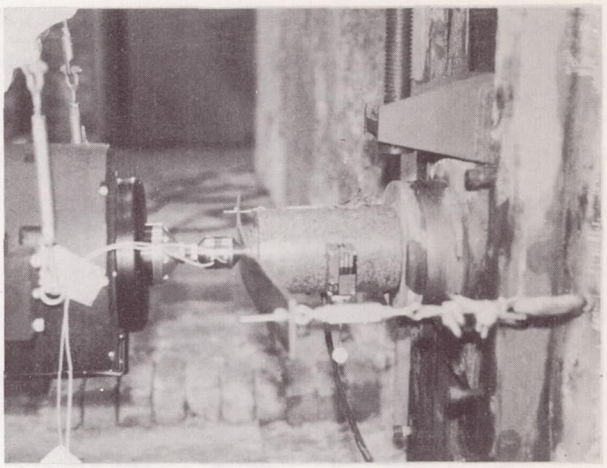

Figure 12—Test configuration for thrust cell measurements.

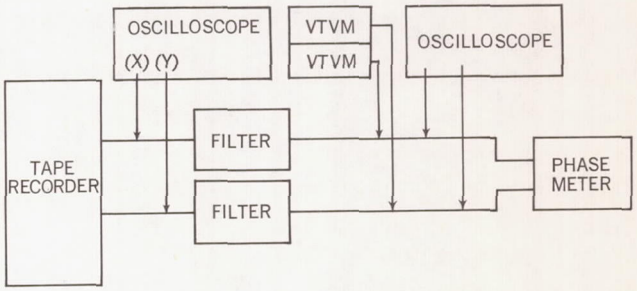

Figure 13—Instrumentation diagram for data analysis.

CONCLUSIONS

From this initial study of the static firing arrangement, at least two points should be noted:

1. The thrust cell acts as a stiff spring below resonance, encouraging acceleration in the higher frequencies while subduing those in the lower frequencies. This tendency exists whenever a thrust cell is used.

2. The X-259 roll-rig assembly contributes an exceedingly soft spring constant that is not completely defined but that must exist at or near the normal point of thrust cell attachment where an oil bearing surface is known to exist.

The resonance of the unloaded thrust cell at 3 kc is not in itself significant, but the possibility and almost certain existence of a lower natural frequency under load must be fully recognized. A mass load of only 150 lb would bring this resonant frequency down into the 500 cps region, which can be extremely critical when resonant burning problems exist. Tentative evidence already points to a correlation between propellant mass decrease versus time and the time after ignition at which certain resonant burning conditions are initiated.

For roll-rig firings, the soft-spring-constant characteristic introduces a very low impedance to the motor and tends to reinforce the higher frequencies to an even greater degree than the thrust cell; however, the large mass of the thrust adapter and oil bearing guides may considerably diminish this effect.

Since this preliminary study has been most encouraging, a more intensive study of the X-259 and X-248 rocket motors is presently in progress, and a continuing investigation with constant improvement in instrumentation and techniques is planned.

ACKNOWLEDGMENT

The wholehearted cooperation of Allegany Ballistics Laboratories, in particular the generous assistance of Mr. Claude Rutherford, in the performance of the field tests is gratefully acknowledged.

Appendix A

An Introduction to Mechanical Impedance and Apparent Weight Concepts

Introduction

Impedance is by definition a measure of the responsiveness of an element to some external excitation. *Mechanical Impedance* is a measure of the mechanical system's response (motion) to an applied excitation (force). It is exactly equal to the ratio of the applied force to the resulting velocity at a point (or what may be assumed to be a point) in a structure.* Thus a system (or element), to have a high impedance, requires large forces to set it in motion, that is, to give it a velocity; and, to have a low impedance, a system requires only small forces to achieve high velocities. In dynamics remember that we are primarily concerned with sinusoidal functions of force and velocity and that in mechanical impedance studies the further limitation of having only steady-state sinusoids is often assumed in order that we may work in the frequency domain rather than in the time domain.†

Another dynamic relation follows from the definition of impedance (since we assumed only that a ratio of excitation to motion was required); this is the *Apparent Mass* relation, equal to force divided by acceleration. Since acceleration in dynamics is most often used in terms of g's, this term is commonly referred to as the *Apparent Weight,* so called because the apparent weight presented by a mass at low frequencies is equal to its weight. The apparent weight concept seems the most natural of the two and, in most cases, is the simplest to acquire with laboratory instruments. Fortunately these two phenomena are related simply, as will be seen, and either may be used to derive the other as the situation demands.

The mechanical impedance or apparent weight concepts, then, define the dynamic behavior at a point in a system or element that meets certain requirements, the most important of which is that the device be composed of linear, bilateral element(s) that can be considered to act in a straight line.‡

Symbols and Mechanical Elements

The symbols and mechanical elements used herein are defined as follows:

A acceleration (g's)§

D viscous damping (lb/in./sec), units mt^{-1}

F force (lb),§ mlt^{-2}

*Assuming of course that proper units of length l mass m, and time t are chosen; and keeping in mind that all variables will be assumed to be rotating vectors, i.e., contain both a real and an imaginary part.

†This limitation is being applied for the present discussion, and is in no sense required by the impedance concept.

‡For a discussion of these limitations, refer to the literature recommended at the end of the Discussion section.

§Unless otherwise stated, a vector quantity.

f_n natural frequency (cps), t^{-1}

g gravitational constant equal to 32.2 ft/sec^2, lt^{-2}

j indicates an angular advancement of +90 degrees

k spring constant (lb/in.), mt^{-2}

M mass (lb mass), mlt^{-2}

V velocity (ft/sec),* lt^{-1}

W_a apparent weight (lb),* mlt^{-2}

$\angle W_a$ phase angle of the vector or angle by which F leads A

Z mechanical impedance,* mt^{-1}

$\angle Z$ phase angle of the vector or angle by which F leads V

ω angular frequency (radians/sec), t^{-1}


damper D


spring k

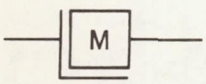

mass M

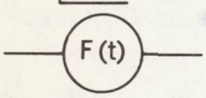

force generator F(t)


fixed reference plane (the earth)

Discussion

Of the many mechanical elements available, three of the most important are discussed here: damping (viscous), mass, and spring.

Damping—The viscous damper D is normally rated in pounds per foot per second and hence is a constant impedance:

$$Z = \frac{F}{V} = D . \qquad \text{(A1)}$$

*Unless otherwise stated, a vector quantity.

Mass—The relation between force and motion for a mass F = MA allows the determination of the ratio of F/V by the following procedure:

Let

$$F(t) = F_0 e^{j\omega t} .$$

Then

$$A(t) = \frac{F_0 e^{j\omega t}}{M} ,$$

and

$$V(t) = \frac{1}{M}\int F_0 e^{j\omega t} dt ;$$

or

$$V(t) = \frac{F_0}{j\omega M} e^{j\omega t} ,$$

and finally,

$$Z = \frac{F}{V} = j\omega M . \tag{A2}$$

Spring—In a similar manner the impedance of the spring is

$$Z = \frac{k}{j\omega} . \tag{A3}$$

With the establishment of the above three equations, we need only to set up the ground rules whereby the combination of elements in systems may be reduced by mathematical manipulations to determine the magnitude and phase of Z.

There are basically only two types of circuits or interconnections to consider: the series, and the parallel. The series circuit is indicated whenever two elements are so arranged that the forces acting on each of them must be identical (as illustrated by Example 2, which follows this discussion). The parallel circuit is simply the inverse of this and is evidenced by the fact that the forces need not be equal; however, the velocity drops* across the elements (as seen in Example 1) will be equal. The rules for combining elemental impedances for these two conditions are as follows:

*The velocity drop across an element is simply the force acting on the element divided by the impedance, or V = F/Z.

I - Elements in series present an impedance Z as:

$$\frac{1}{Z_{total}} = \frac{1}{Z_1} + \frac{1}{Z_2} + \frac{1}{Z_3} + \cdots + \frac{1}{Z_n} .$$

II - Elements in parallel present an impedance Z as:

$$Z_{total} = Z_1 + Z_2 + Z_3 + \cdots + Z_n .$$

Since any combination of impedance, regardless of complexity, may be viewed step by step as either a series of parallel combination of two or more elements, any circuit may be reduced by the above rules to a single impedance consisting of a real component (if damping is present) and an imaginary component.

The relation between Z and W_a may be derived by using the known relation between velocity and acceleration:

$$A = j\omega V ,$$

and

$$W_a = \frac{F}{A} = \frac{F}{j\omega V} ;$$

then

$$W_a = \frac{Z}{j\omega} .$$

In order to emphasize the foregoing rules and conclusions, three solutions to simple mechanical circuits are illustrated and analyzed on the following pages. The literature cited below is recommended for a more thorough discussion of this subject.

A1. Firestone, Floyd A., "American Institute of Physics Handbook," New York: McGraw Hill Book Co., 1957.

A2. Olson, Harry F., "Dynamical Analogies," New York: D. Van Nostrand, 1943.

A3. Mason, W. P., "Electromechanical Transducers and Wave Filters," Princeton, N. J.: D. Van Nostrand, 1948.

A4. Bradley, Wilson, Jr., "Mechanical Impedance Testing," in *Proc. Institute of Environmental Sciences National Meeting April 1960,* p. 535.

Example 1

The first example to be considered is a spring-mass combination (see Figure A1) with one side of the spring rigidly mounted to a fixed plane. The point at which the spring is attached to the mass is also the point of force application. However, it is to be noted that this excitation may be applied to any part of the mass as long as our previous assumption of linear motion holds, since the mass element may be considered dimensionless physically [Figure A1(a)]. The circuit is analyzed with and without damping to illustrate this effect. Since the velocity of all masses is referred to ground, all masses will have a connection similar to that of Figure A1(b), where the viscous damper could be applied across either the mass or the spring with the same resulting effect.

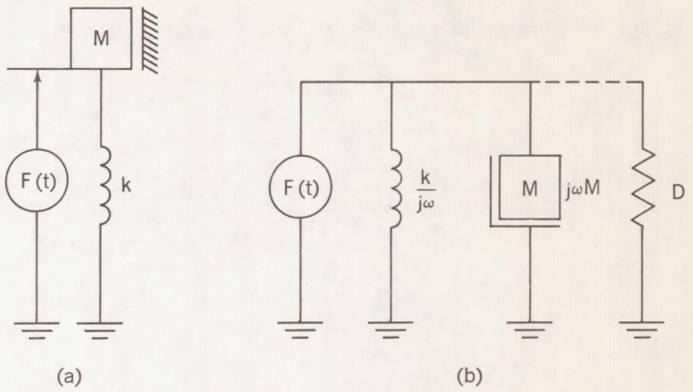

Figure A1—Spring-mass system (a) Mechanical circuit (b) Impedance circuit.

The impedance may be solved by using Equations A1, A2, and A3 and the rule for parallel combination:

A. Without damping,

$$Z = j\omega M - \frac{jk}{\omega} .$$

B. With damping,

$$Z = D + j\omega M - \frac{jk}{\omega} .$$

It is often of interest to know the low and high frequency tendencies of a system, and these may be readily found by letting ω approach zero or infinity in the above equations.

Using case B, with damping, gives

$$\underset{f\to 0}{Z} = D - \frac{jk}{\omega} , \tag{A4}$$

$$\underset{f\to \infty}{Z} = D + j\omega M . \tag{A5}$$

At resonance the reactive terms cancel, and

$$\underset{f=f_n}{Z} = D . \tag{A6}$$

Using the previously found relation,

$$W_a = \frac{Z}{j\omega} ,$$

W_a may be directly written as

$$\underset{f \to 0}{W_a} = \frac{D}{j\omega} - \frac{k}{\omega^2} , \tag{A4a}$$

$$\underset{f \to \infty}{W_a} = \frac{D}{j\omega} + M , \tag{A5a}$$

and

$$\underset{f = f_n}{W_a} = \frac{D}{j\omega} . \tag{A6a}$$

With these asymptotic forms of the impedance function and specially designed graph paper, both Z and W_a may be plotted as one curve and read directly from the graph in Figure A2.

As Equations A4, A5, and A6 indicate, the impedance function follows a spring constant line below resonance and a constant mass (or apparent weight) above resonance. The region near resonance is influenced by the Q of the circuit, defined as

$$Q = \frac{2\pi E}{\Delta E} ,$$

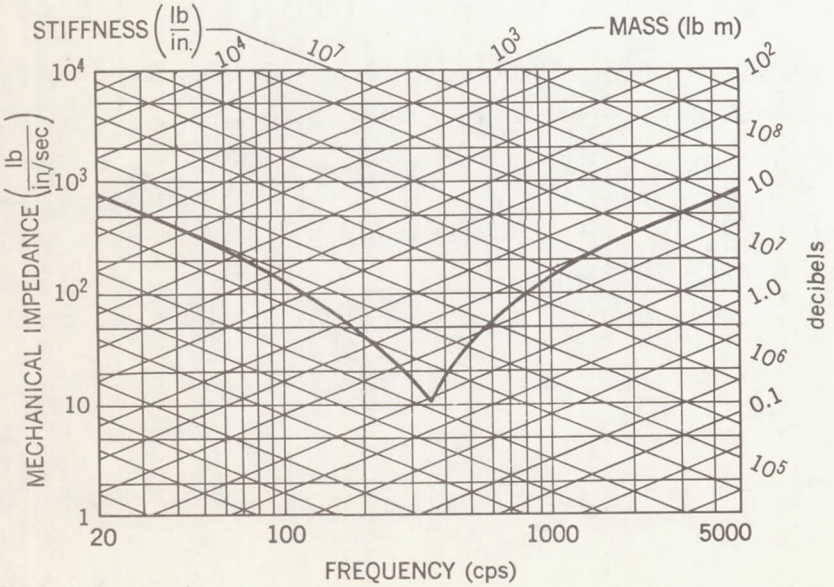

Figure A2—Impedance and apparent weight (Figure A1) vs. frequency.

where E is the energy stored and ΔE is the energy dissipated per cycle.

At resonance the impedance value is exactly equal to the damping D.

The phase angles of Z and W_a may also be sketched to give a more complete picture of the response. In the curves below (Figure A3) it can be seen that the only time Z has a significant real part is at resonance or $f=f_n$, while W_a has a very large real part (phase angle equal to zero) for all frequencies significantly above f_n. This indicates that the mechanical system appears masslike at high frequencies because of the spring's ineffectiveness.

Example 2

Another configuration of interest is the antiresonant arrangement of Figure A4 below.

The impedance of this circuit may be solved by again using Equations A1, A2, and A3 and the rules for series and parallel combination:

C. Without damping,

$$Z = \frac{j\omega Mk}{k - \omega^2 M} .$$

D. With damping,

$$Z = \frac{Dk^2}{k^2 - \omega^2(2Mk - D^2) + \omega^4 M^2} + j\omega \frac{Mk(k - \omega^2 M) - D^2 k}{k^2 - \omega^2(2Mk - D^2) + \omega^4 M^2} .$$

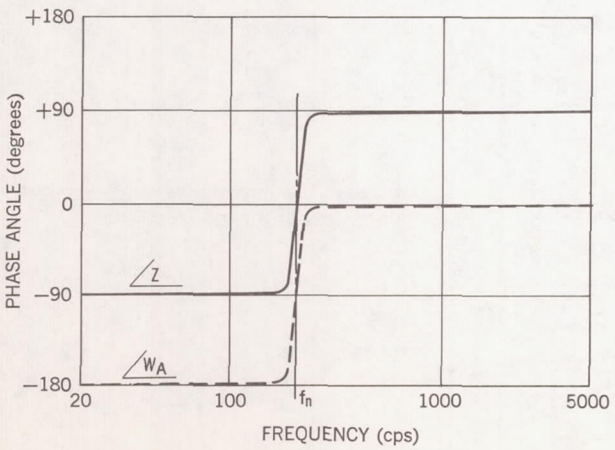

Figure A3—Phase angle of Z and W_a vs. frequency.

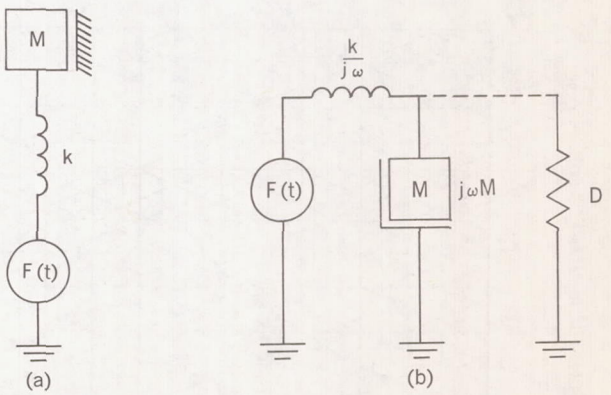

Figure A4—A driven spring-mass system (a) Mechanical circuit (b) Impedance circuit.

The frequency spectrum of Z and W_a may again be found by studying the high and low frequency asymptotes of Z and the antiresonant conditions for cases C and D.

Using case D, which includes damping, gives

$$\underset{f\to 0}{Z} = D + j\omega M , \tag{A7}$$

$$\underset{f\to \infty}{Z} = \frac{k}{j\omega} + \frac{Dk}{M} , \tag{A8}$$

and

$$\underset{f=f_n}{Z} \cong \frac{Mk}{D} . \tag{A9}$$

The apparent weight relations can again be written from Equations A7, A8, and A9 as

$$\underset{f\to 0}{W_a} = M + \frac{D}{j\omega} ,$$

$$\underset{f\to \infty}{W_a} = \frac{Dk}{j\omega M} - \frac{k}{\omega^2} ,$$

$$\underset{f=f_n}{W_a} = \frac{Mk}{j\omega D} .$$

The magnitude of both Z and W_a peak up at antiresonance as expected (Figure A5).

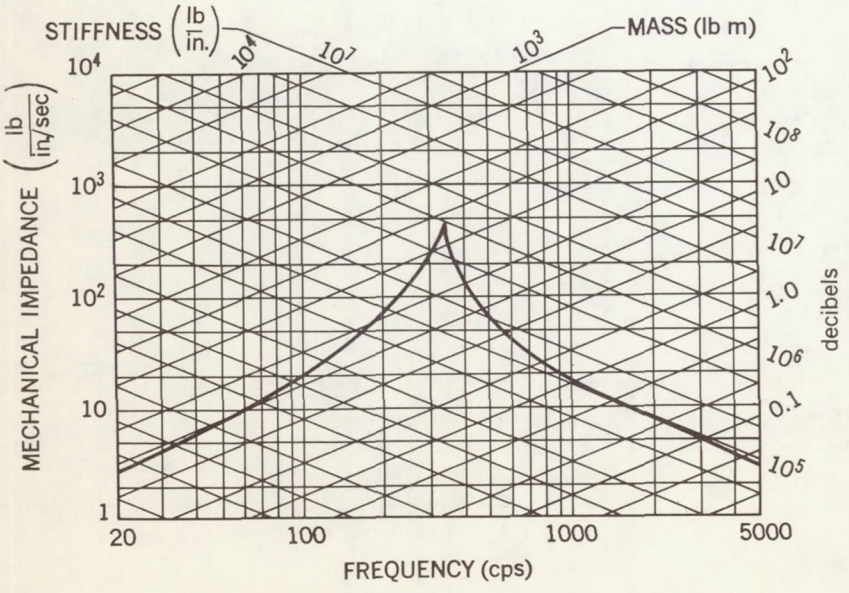

Figure A5—Impedance and apparent weight vs. frequency.

The phase angles also may be of interest and may be approximated from the impedance equations. The degree of approximation is dependent on the degree of damping, but of course these equations may be solved very easily for any desired degree of accuracy.

The Figure A6 plot shows the phase shift passing through antiresonance but, most importantly, note that the phase angles at antiresonance are identical for both Z and W_a, as they were for resonance (see Figure A3).

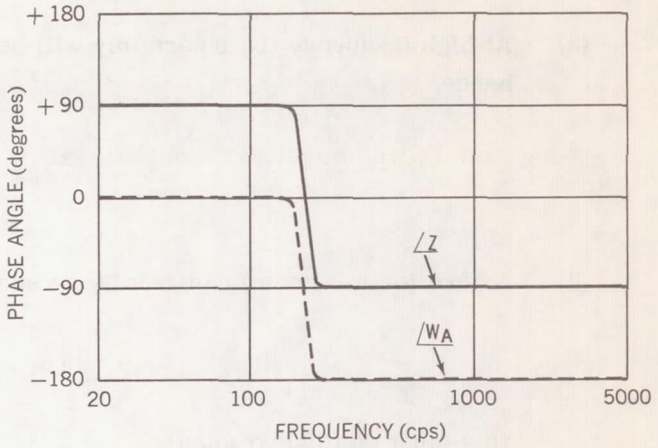

Figure A6—Phase angles of Z and W_a vs. frequency.

Example 3

The final circuit to be considered, Figure A7, contains properties similar to both of the preceding circuits and shows important aspects of both resonance and antiresonance not strictly deduceable from the previous two illustrations.

The circuit consists of two masses separated by a spring, with the forcing function F(t) acting on one of the masses.

For this problem we will discuss only the impedance function Z, since by now the transformation to W_a is obvious.

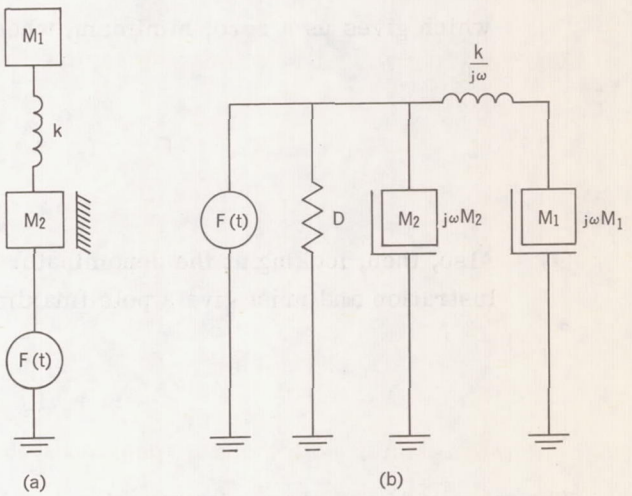

Figure A7—Complex mechanical system (a) Mechanical circuit (b) Impedance circuit.

$$Z = D + j\omega M_2 + \frac{j\omega M_1 \times \frac{k}{j\omega}}{\frac{k}{j\omega} + j\omega M_1},$$

which reduces to

$$Z = D + j\omega \frac{kM_1 + kM_2 - \omega^2 M_1 M_2}{k - \omega^2 M_1}.$$

When the impedance function is written in the above form, the frequency characteristics often may be derived simply by contemplating this equation in the following steps:

(1) At low frequency the ω factor in the numerator will tend to zero, or

$$\underset{f \to 0}{Z} \approx D + j\omega(M_1 + M_2).$$

(2) At high frequency the D certainly will become insignificant, and the ω^2 terms will dominate; hence,

$$\underset{f\to\infty}{Z} \approx j\omega M_2 .$$

(3) A zero (or minimum) can readily be seen in the numerator by looking at the term

$$\left(kM_1 + kM_2 - \omega^2 M_1 M_2\right) ;$$

this must go to zero when

$$k\left(M_1 + M_2\right) = \omega^2 M_1 M_2 ,$$

which gives us a zero, minimum, when

$$f = f_0 = \frac{1}{2\pi}\sqrt{\frac{k\left(M_1 + M_2\right)}{M_1 M_2}} .$$

(4) Also, then, looking at the denominator we see that it is similar to case C of our second illustration and must give a pole (maximum) of impedance when

$$f = f_x = \frac{1}{2\pi}\sqrt{\frac{k}{M_1}} .$$

The magnitude and phase of Z may then be sketched as before (Figure A8).

The peak-notch effect is clearly present in Figure A8(a). It is caused essentially by the fact that a series resonance between k and M_1 is present, as well as a possible parallel antiresonance between k and M_2. The relation between f_x and f_0 may be found as follows:

$$f_0 = \frac{1}{2\pi}\sqrt{\frac{k}{M_1} + \frac{k}{M_2}} .$$

From this last expression it follows that, for $M_2 >> M_1$, f_0 approaches f_x and the peak-notch effect becomes extremely sharp and, for $M_2 \cong M_1$, $f_0 = \sqrt{2} f_x$. Also, for $M_2 << M_1$, $f_0 \to \infty$.

In Figure A8(b) it is important to note that, as the frequency varies through both f_0 and f_x, the phase angle of Z passes through 0 degrees. It is significant that the phase angle between f_0 and f_x need not reach −90 degrees but, for our considerations, it *must* pass through zero.

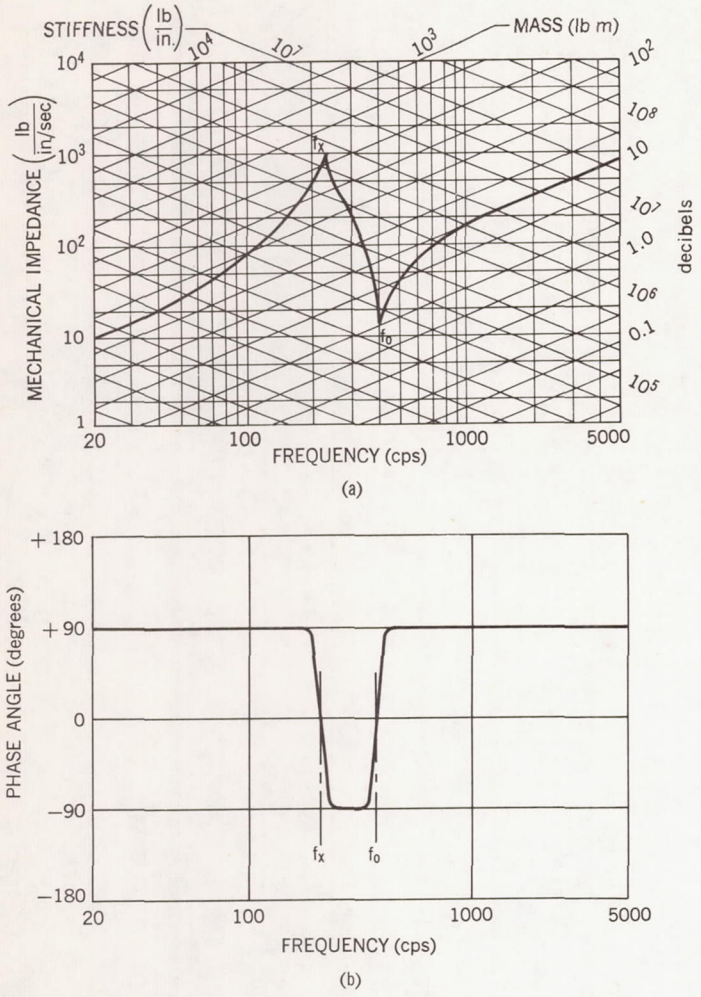

Figure A8—Typical frequency response of Figure A7 (a) Impedance vs. frequency (b) Phase angle of Z vs. frequency.

Some very important facts can be drawn from the foregoing data and curves, namely:

1. When the phase angle of the apparrent weight W_a is near zero degrees, the system is masslike; that is,

$$W_a \approx M .$$

2. When the phase angle of W_a is near 180 degrees, the system is springlike; or

$$W_a \approx -\frac{k}{\omega^2} .$$

3. When the phase angle of W_a is -90 degrees, the system is at resonance if $d\angle W_a / df$ is positive, and is at antiresonance if $d\angle W_a / df$ is negative.

4. If the system does not depart from our previous assumptions of linearity, etc., the $\angle W_a$ must lie in quadrants 3 and 4 only.

These rules of thumb are extremely valuable in the interpretation of impedance and apparent weight data.